Advanced Steel Construction 2 (2006) 1-21

MONOTONIC AND CYCLIC TESTS ON SHEAR DIAPHRAGM DISSIPATORS FOR STEEL FRAMES

M.S. Williams[1] and F. Albermani[2]

[1]*University of Oxford, UK, Email: martin.williams@eng.ox.ac.uk*
[2]*University Of Queensland, Australia, Email: f.albermani@uq.edu.au*

Abstract: This report describes a series of cyclic tests on a yielding shear panel device. The device consists of a short length of square hollow section (SHS) with a diaphragm plate welded inside it. It is positioned between the braces and the main members of a braced frame, with the diaphragm lying in the plane of the frame, so that it is loaded in pure shear as the frame undergoes lateral deformation. An extensive series of tests on 100 mm square dissipative devices mounted in a single-storey, planar, K-braced frame was successfully performed, under both monotonic and cyclic loads.

The devices proved easy and cheap to manufacture, fit, remove and replace. All the devices tested yielded at quite low deformations and sustained very large ductilities without failure. The load carried by the device continued to increase after yield, with a ratio of maximum force carried to yield force of around 1.7 in most tests.

While a device with a 2 mm diaphragm appeared to offer the maximum energy dissipation capacity, thinner devices were prone to buckling and to fracture under repeated, large-amplitude cycling. A thickness of 3 mm (i.e. thickness to breadth ratio of 0.03) is recommended as offering the best combination of dissipative capacity and robustness. A 3 mm device dissipated approximately 1.3 kJ of energy when the frame in which it was fitted underwent a single displacement cycle of amplitude 30 mm.

It is concluded that these devices offer a simple, cheap and robust way of dissipating significant amounts of energy in seismically loaded frames. Some improvements to the rig design and suggestions for further work are offered in section 4.6.

Keywords: seismic retrofitting, energy dissipative device, shear panel

1. INTRODUCTION

This report describes a series of cyclic tests on a yielding shear panel device of the form proposed by U. Dorka (unpublished) at the University of Kassel, Germany. Tests on similar devices, but using different techniques, are currently being performed at the EU Joint Research Centre at Ispra, the National Technical University at Athens, LNEC Lisbon and the University of Oxford, as part of the EU-funded Neforeee research programme (Blackeborough *et al.*, 2001).

The device consists of a short length of square hollow section (SHS) with a diaphragm plate welded inside it. The device is positioned between the braces and the main members of a braced frame, with the diaphragm lying in the plane of the frame, so that it is loaded in pure shear as the frame undergoes lateral deformation. Energy is dissipated through shear yielding of the diaphragm, which is restrained from buckling by the surrounding SHS. Tests are reported on devices mounted in a single-storey planar braced frame, under both monotonic and ramped, reverse-cyclic loads.

2. TEST RIG DESIGN

The devices were tested in a single-storey, planar, K-braced frame constructed at approximately half of prototype scale, so as to fit into an existing loading frame. A general arrangement and details of the frame is shown in Figure 2.1. The device design was based around a section of 100 × 100 × 4 SHS with a welded diaphragm thickness of up to 6 mm. Taking the tensile yield strength of the diaphragm as 300 MPa, the shear modulus as 80 GPa and incorporating an overstrength factor of 1.2 gives the following values of maximum shear yield force, elastic stiffness and yield deformation of the device:

$$F_y = 1.2 \times \frac{300}{2} \times 100 \times 6 = 108 \text{ kN}$$

$$k_e = \frac{80 \times 100 \times 6}{100} = 480 \text{ kN/mm}$$

$$u_y = \frac{F_y}{k_e} = 0.225 \text{ mm}$$

Thinner diaphragm plates would be expected to have proportionately smaller yield loads and elastic stiffnesses, but the same yield deformation.

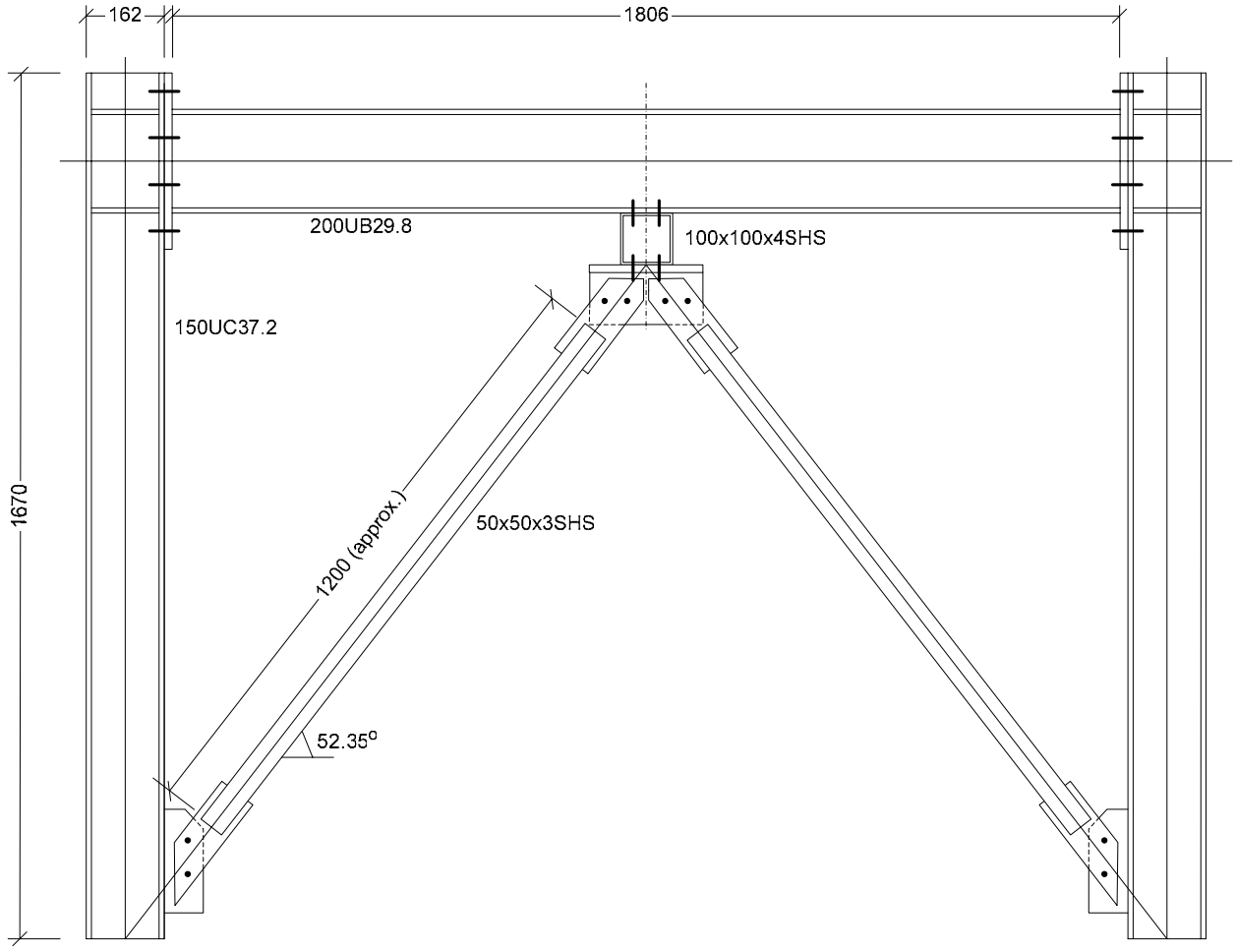

Figure 2.1. Dissipative Device Test Frame – General Arrangement

The remainder of the frame was designed to remain elastic at a lateral load of up to 200 kN. Non-linear static analysis of the frame was performed using Mastan, a simple frame analysis program written in Matlab (Zieman and McGuire, 2000). The device was represented by an elastic-plastic link element with the properties given above. Members and connections were designed in accordance with the Australian steelwork code (AS 4100, 1990), using section properties and material strengths supplied by OneSteel (2003). The results of the analyses indicated that, with a 6 mm diaphragm, device yield would occur at a lateral load of approximately 125 kN and a cap-beam lateral displacement of around 2 mm. Under continued monotonic loading the frame would carry a total load of around 200 kN at a lateral displacement of approximately 9 mm.

3. TEST PROCEDURE

3.1. Test Setup and Instrumentation

The test setup is shown in Figures 3.1 and 3.2. Due to limitations in the support frame available, the test structure was rotated through 90° for testing, with the bases of the columns mounted on one of the verticals of the support frame. Load was applied by a 250 kN capacity hydraulic actuator mounted on the top beam of the support frame and acting along the centreline of the cap beam of the test structure. The instrumentation comprised:

- a 220 kN tension/compression load cell mounted between the actuator and the test frame
- two cable extension transducers to measure the displacements at the centreline of the cap beam and at the top of the braces, immediately below the dissipative device
- strain gauges on the two diagonal braces to enable their axial forces to be determined. An average strain reading from opposite faces of each brace was taken, so as to eliminate the effects of any unintended bending
- dial gauges positioned on the support frame adjacent to the column bases, to monitor any possible base movement

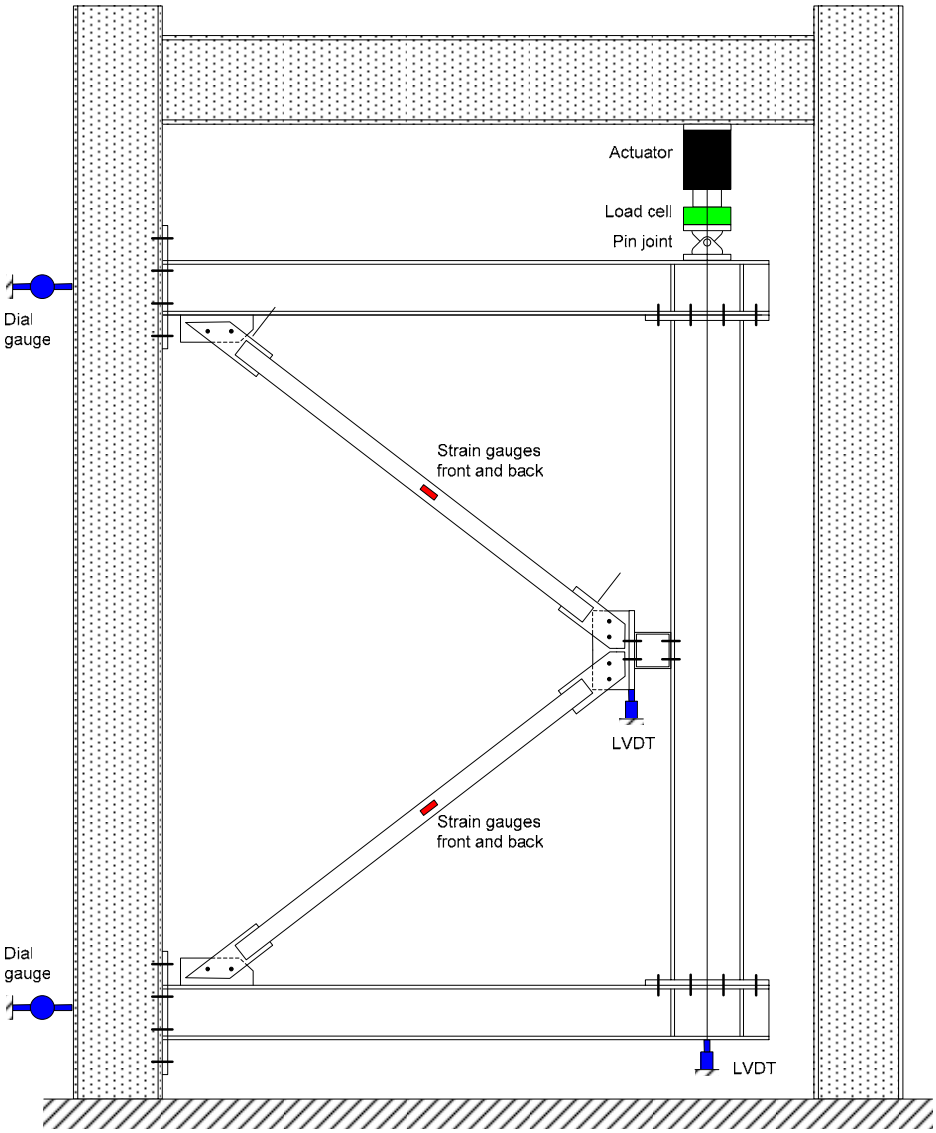

Figure 3.1. Test Setup and Instrumentation

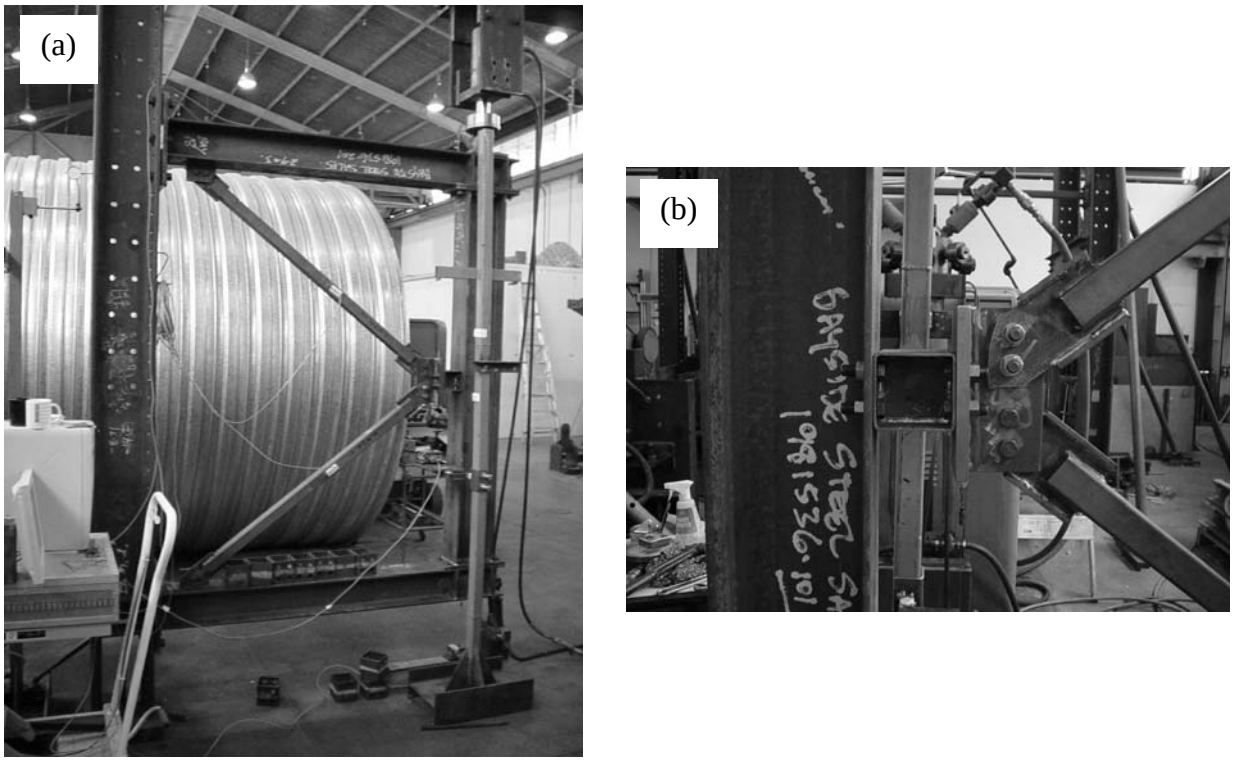

Figure 3.2. Test setup – (a) general layout and (b) device connection detail

The orientation of the test structure raised the possibility that gravity loads might cause some initial sway deformation which would not be measured. To prevent this, the following setup procedure was adopted. Strain gauge zero readings were taken with the braces under zero load. The braces were then bolted in place and the cap beam pulled upwards until the strain gauges returned to their zero readings. The actuator was then locked in position and zero readings of all other instruments were taken.

Tests were performed under several different loading regimes. For each diaphragm plate thickness, the first test comprised a simple, monotonically increasing load up to failure, in order to determine the device's yield point and its ultimate capacity. Ramped reverse-cyclic tests were then performed following the schematic pattern shown in Figure 3.3, with the variation in the number of cycles n at each amplitude intended to assess the vulnerability of the device to low cycle fatigue.

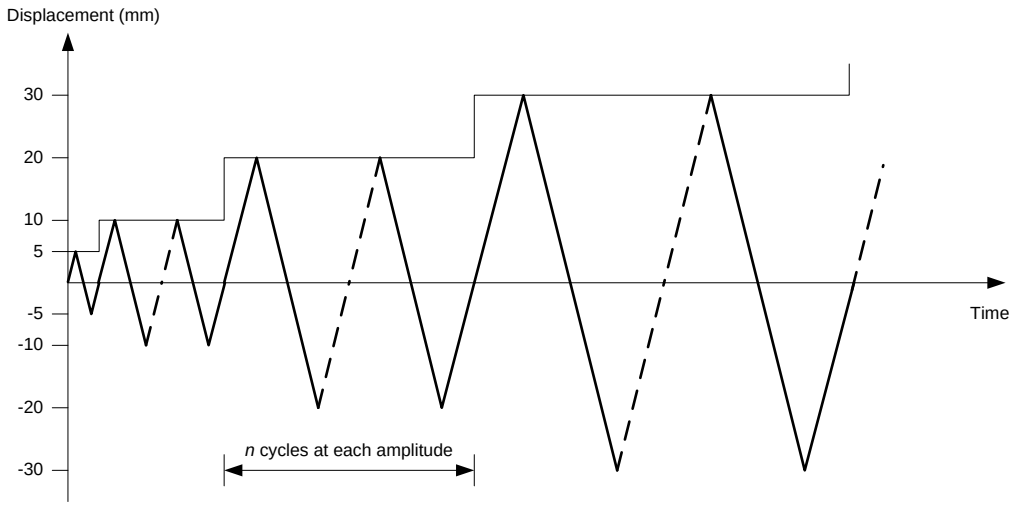

Figure 3.3. Schematic of cyclic loading regime

Tables 3.1 and 3.2 summarise all the tests performed.

Table 3.1. Summary of test programme (cell entries in last three columns show test numbers)

Plate thickness (mm)	Single or double plate	Monotonic test	Cyclic test (single cycle at each amplitude)	Cyclic test (three cycles at each amplitude)
1	Double	4	7	–
1.5	Double	5	8	–
2	Double	1,2	3,6	14
1	Single	9	10	16
1.5	Single	11	12	15
2	Single	18	19	20
3	Single	21	22	23
4	Single	13	24	–
No plate	–	–	17	–

Table 3.2. Details of tests performed

Test no.	Diaphragm thickness (mm)	σ_y (MPa)	Test type	n	Max. disp. (mm)	Max. load (kN)
Free1	–	–	Cyclic	1	41.7	124.4
Free2	–	–	Cyclic	1	40.3	118.9
1	2 × 2	260	Monotonic	–	37.7	205.1
2	2 × 2	260	Monotonic	–	32.0	176.6
3	2 × 2	260	Cyclic	1	40.2	184.6
4	2 × 1	190	Monotonic	–	34.0	118.5
5	2 × 1.5	332	Monotonic	–	50.0	191.0
6	2 × 2	260	Cyclic	1	40.9	161.0
7	2 × 1	190	Cyclic	1	30.4	121.9
8	2 × 1.5	332	Cyclic	1	40.4	149.7
9	1	200	Monotonic	–	34.3	94.8
10	1	200	Cyclic	1	30.1	103.9
11	1.5	332	Monotonic	–	45.5	135.6
12	1.5	332	Cyclic	1	43.5	134.7
13	4	300	Monotonic	–	55.2	183.2
14	2 × 2	260	Cyclic	3	38.9	143.8
15	1.5	332	Cyclic	3	32.6	111.5
16	1	200	Cyclic	3	30.2	99.2
17	No plate	–	Cyclic	1	29.9	84.8
18	2	260	Monotonic	–	41.1	125.4
19	2	260	Cyclic	1	40.5	142.9
20	2	260	Cyclic	3	31.5	117.3
21	3	285	Monotonic	–	51.2	159.5
22	3	285	Cyclic	1	40.2	151.5
23	3	285	Cyclic	3	30.4	119.1
24	4	300	Cyclic	1	40.3	158.8

3.2. Conduct of Tests

In general the conduct of the tests was straightforward. However, a few minor changes were made as the tests proceeded, to reduce perceived errors.

Initially, the columns were bolted to the support frame using three rows of two bolts, giving a high degree of fixity. In the first test, unexpectedly high loads were achieved and the decision was therefore taken to reduce the support stiffness. This was done by removing all but the middle row of two bolts in each base plate. A further problem was that the base plates then appeared to yield differentially, giving a higher stiffness when pulling up than when pushing down. From test 8

onwards this effect was alleviated but not eliminated by packing the supports using 5mm plates locally around the central line of bolts, as shown in Figure 3.4.

Figure 3.4. Final support arrangement

While it was initially intended to test devices with diaphragms up to 6 mm thick, in the event it was decided to limit the thickness to 4 mm, as it would be possible to impose only very limited ductility on thicker diaphragms with the available test setup. As well as testing single-plate devices, some tests were conducted on devices made up by of two thinner plates positioned next to each other, each welded to the hollow section but not to each other.

Since the brace connections were made with simple black bolts in clearance holes, some slip was inevitable, and indeed desirable in order to ensure that the braces could rotate at their ends and so behave as pin-ended. However, sudden bolt slip did have some detrimental effects on the smoothness of the hysteresis loops for the devices, and these appeared to worsen in some of the later tests as some bolt holes elongated. From test 21 onwards, attempts were made to reduce the slip by clamping sheets of sandpaper between the brace connection plates. This had limited success.

4. RESULTS

4.1. Presentation of Results

In this section results from each test are briefly presented and discussed. In each case, test observations are recorded and force-deformation characteristics for the whole frame and for the device alone are presented. Subsequent sections then present a variety of comparisons and post-processing. First, “free” tests on the portal frame without any device or bracing are presented. The main tests are then presented in the order: monotonic, cyclic (single cycle at each amplitude) and cyclic (repeated cycles). Within each subset, results are presented in order of increasing plate thickness.

4.1.1. Free tests

Test Free1 – no device, two-bolt connection at each support. This test was performed to investigate the cause of the apparently unsymmetrical behaviour of the frame, as observed in the early device tests. It was clear during the tests that the base plates of the columns were becoming curved and making uneven contact with the support. This resulted in the hysteresis curves shown in Figure 4.1.

Test Free2 – no device, packing plates added at supports (see Figure 3.4). The addition of packing plates around the single line of bolts prevented contacted between the main plates and the support frame, and so resulted in a far more symmetrical performance, though still with limited hysteresis at large amplitudes, as can be seen in Figure 4.2.

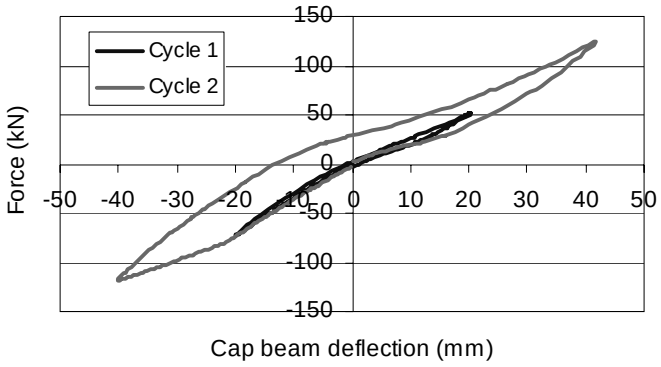

Figure 4.1. Test Free1 – no device

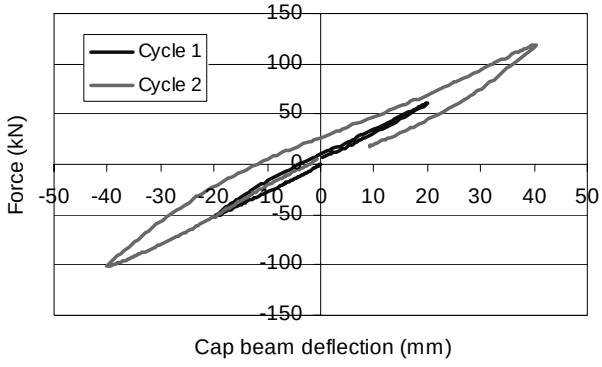

Figure 4.2. Test Free2 – no device

4.1.2. Monotonic tests

1 mm single plate (Test 9). First buckle appeared at a cap beam displacement of approximately 7 mm, corresponding to a device deformation of 2.8 mm. The onset of buckling is not obviously visible in the force-deformation plots of Figure 4.3. Buckles became more pronounced with increasing amplitude but no failure occurred.

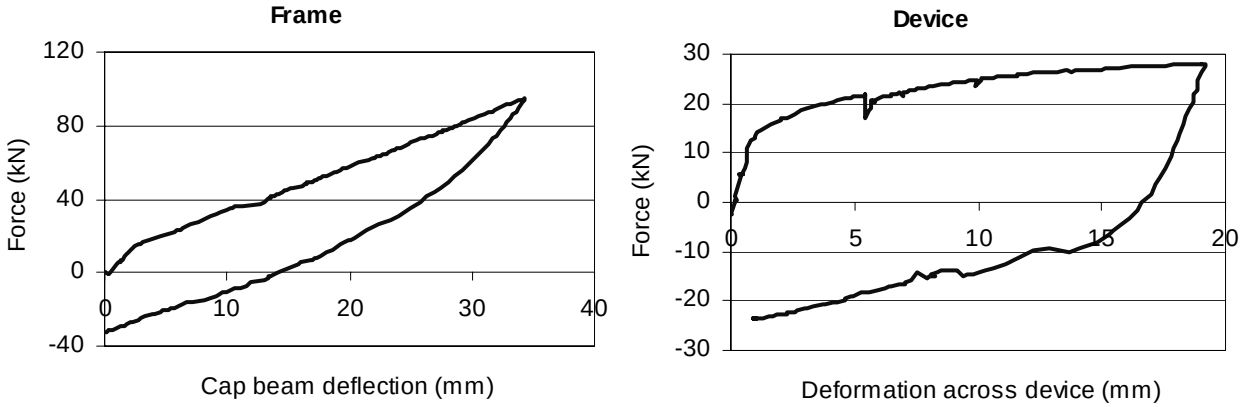

Figure 4.3. Monotonic test, 1 mm single plate

1.5 mm single plate (Test 11). First buckle appeared at a cap beam displacement of 15 mm, at which point the device deformation was around 5 mm.

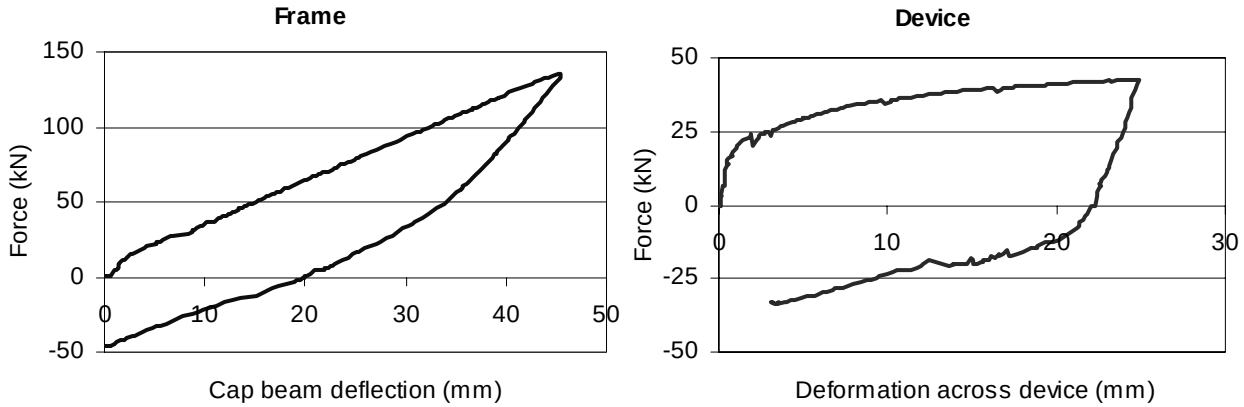

Figure 4.4. Monotonic test, 1.5 mm single plate

2 mm single plate (Test 18). First buckle appeared at a cap beam displacement of 18-20 mm, at which point the device deformation was 9-10 mm.

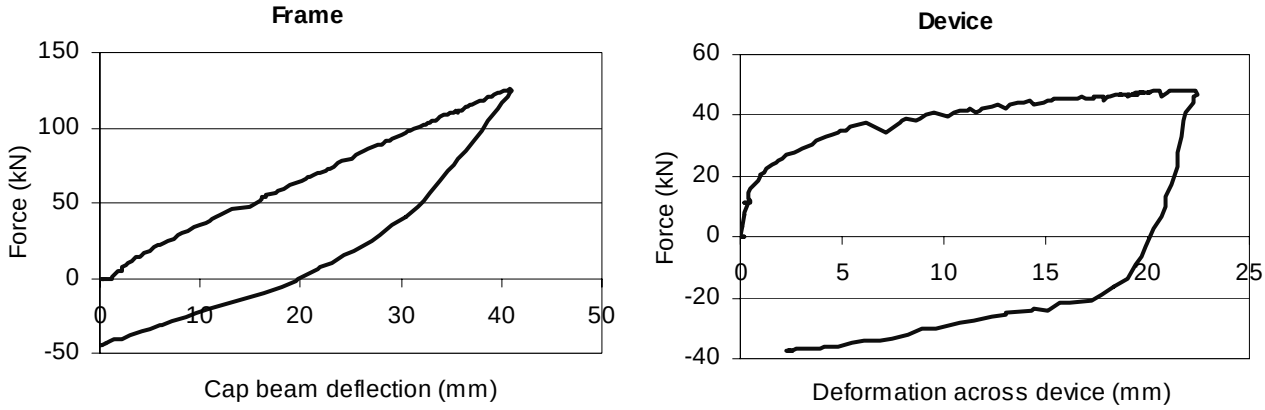

Figure 4.5. Monotonic test, 1.5 mm single plate

2 x 1 mm plates (Test 4). First buckle appeared at a cap beam displacement of around 20 mm, at which point the device deformation was 8 mm.

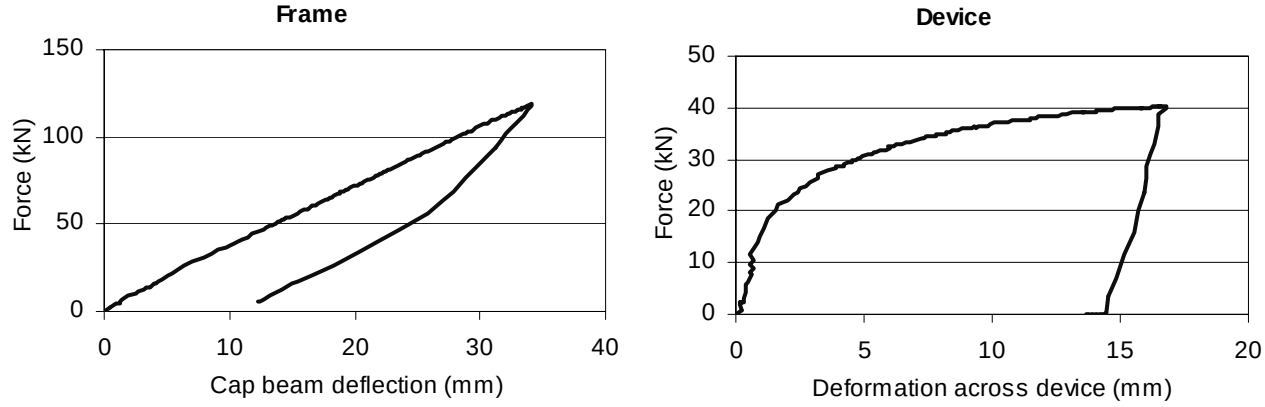

Figure 4.6. Monotonic test, 2 x 1 mm plates

3 mm single plate (Test 21). No apparent buckling at cap beam displacements of up to 50 mm.

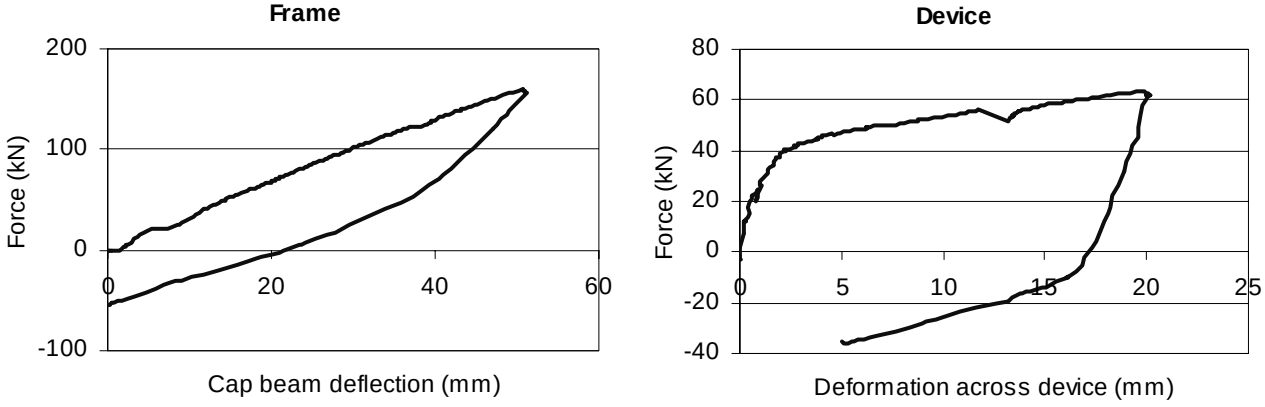

Figure 4.7. Monotonic test, 3 mm single plate

2 x 1.5 mm plates (Test 5). First buckle appeared at a cap beam displacement of around 25 mm, at which point the device deformation was 11 mm. Buckling is not evident in the load-deformation plots of Figure 4.8, which are quite similar to those for a single 3 mm plate, Figure 4.7.

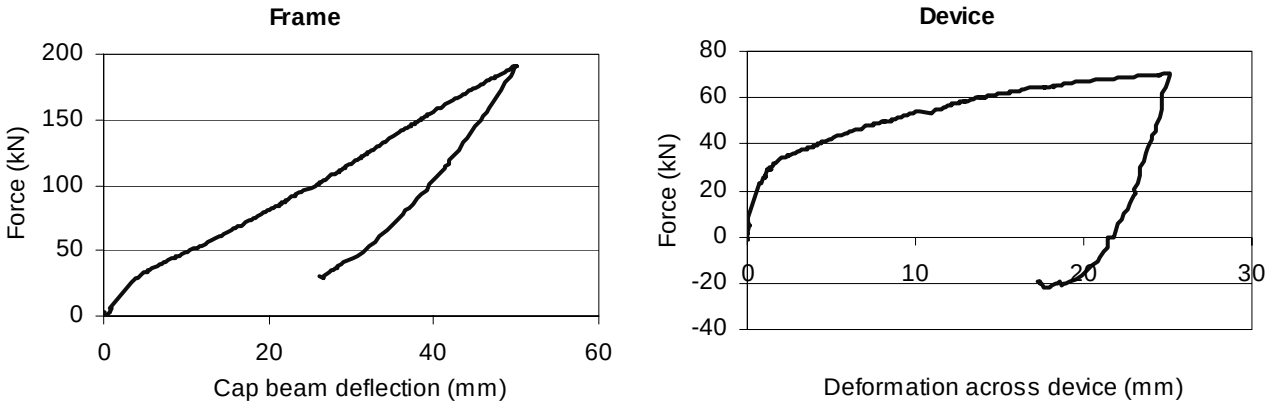

Figure 4.8. Monotonic test, 2 x 1.5 mm plates

4 mm single plate (Test 13). No apparent buckling at cap beam displacements of up to 55 mm. A 60 kN reverse load was required to bring the frame back to zero displacement.

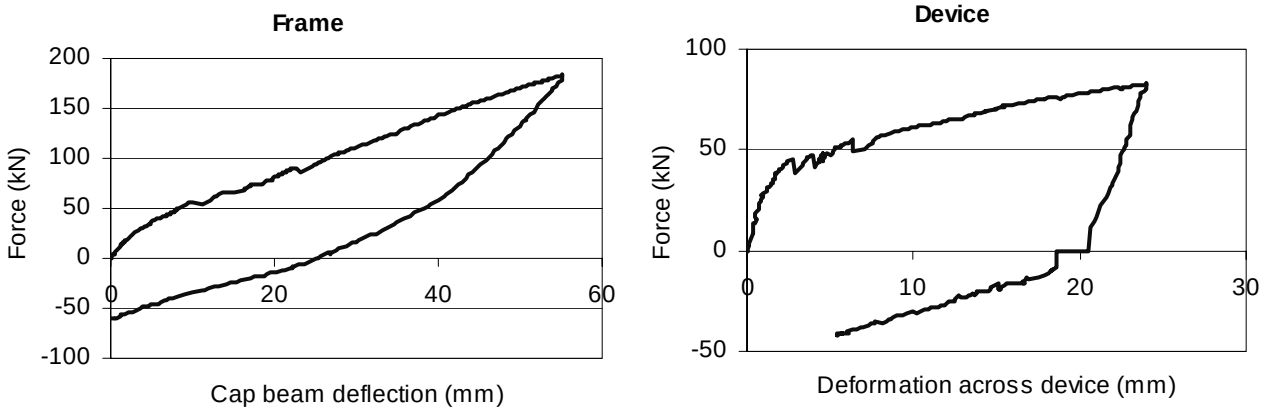

Figure 4.9. Monotonic test, 4 mm single plate

2 x 2 mm plates (Test 2). First buckle appeared at a cap beam displacement of around 25 mm, at which point the device deformation was 10 mm. Buckling is not evident in the load-deformation plots of Figure 4.10, which are quite similar to those for a single 4 mm plate, Figure 4.9. Figure 4.11 shows the device at the point of maximum deformation.

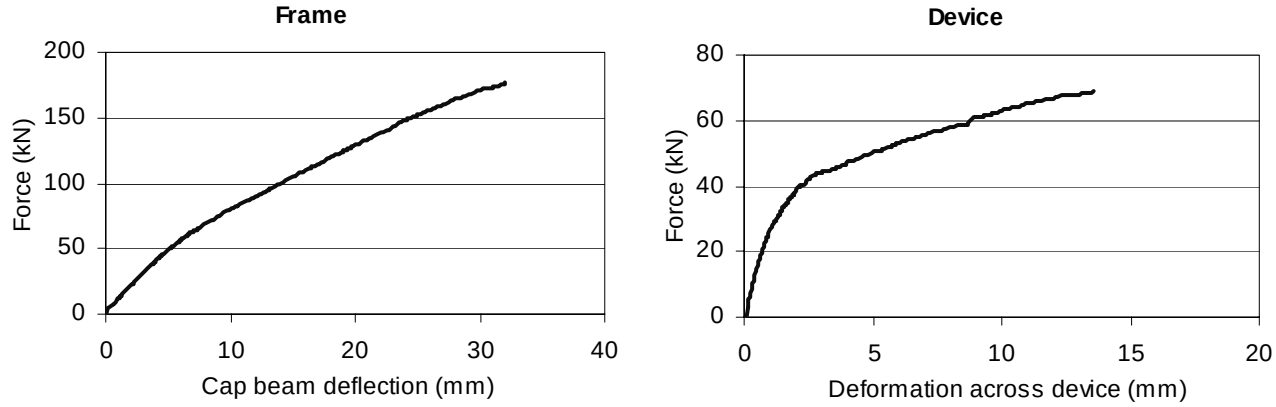

Figure 4.10. Monotonic test, 2 x 2 mm plates

Test 1 was also a monotonic test on two 2 mm plates but is not reported here as it was the only test conducted with fixed column bases, and so is not easy to compare to the others.

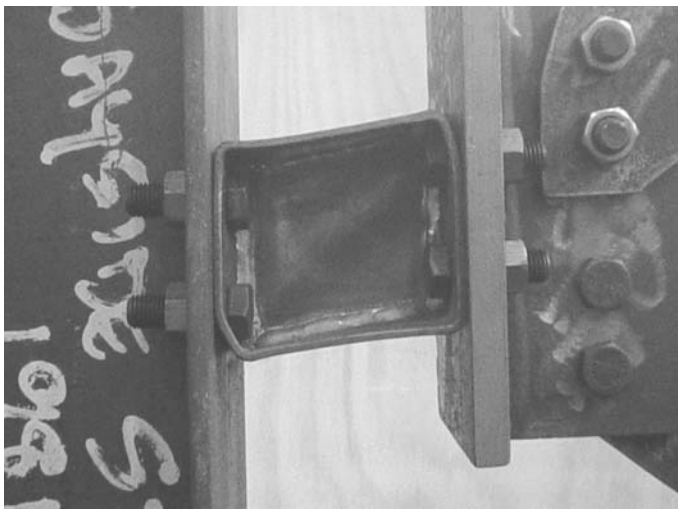

Figure 4.11. 2 x 2 mm plate device at point of maximum deformation

4.1.3. Simple cyclic tests

In these tests a single reverse cycle was imposed at each displacement amplitude.

Open box section – no plate (Test 17). This test was conducted as a control. The device yielded at a very low load and carried no load on the unloading cycle until it had been pushed back past its zero deformation point.

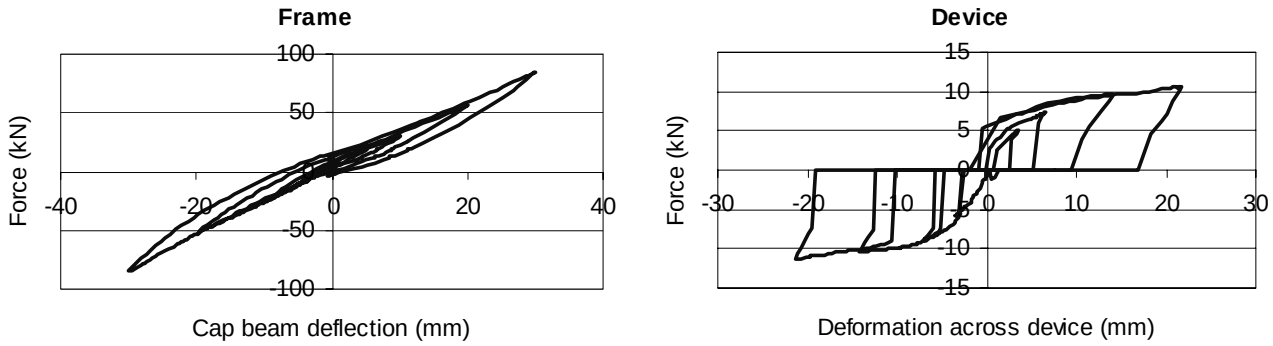

Figure 4.12. Cyclic test – no plate

1 mm single plate (Test 10). A very slight buckle developed during the 5 mm cycle, and amplified in subsequent cycles. The test was discontinued midway through the 30 mm cycle as the buckle amplitude was becoming very large, although the device continued to carry load. The deformations imposed on the device were highly unsymmetrical, with much larger demands on the initial upwards pull (negative quadrant) than in the subsequent downwards push (positive quadrant). It is thought that the large flat region of the device hysteresis curve at zero load when unloading from the negative quadrant is due to flattening out of a buckle. Other minor kinks are due to bolt slip.

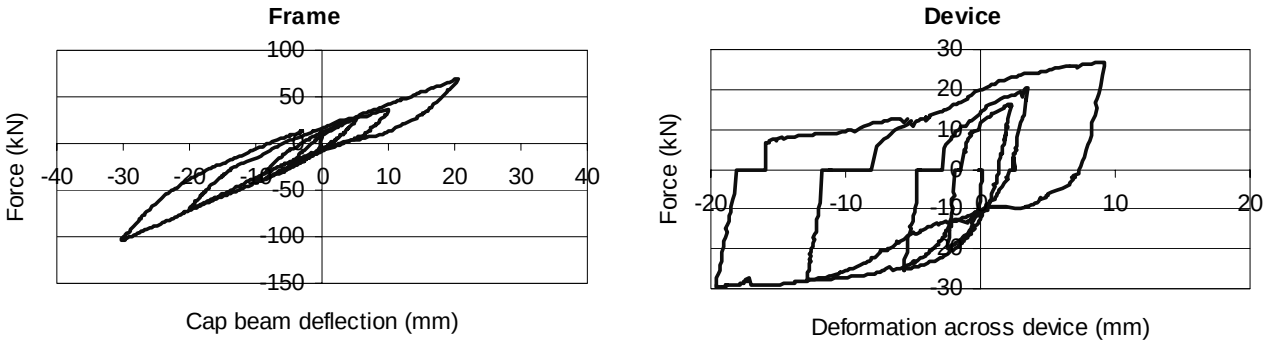

Figure 4.13. Cyclic test – 1 mm single plate

1.5 mm single plate (Test 12). A very slight buckle developed during the 10 mm cycle, and amplified in subsequent cycles. The test was discontinued midway through the 40 mm cycle as the buckle amplitude was becoming very large, although the device continued to carry load. The deformations imposed on the device were again rather unsymmetrical. The device hysteresis curve is in general rather smoother than in Test 10.

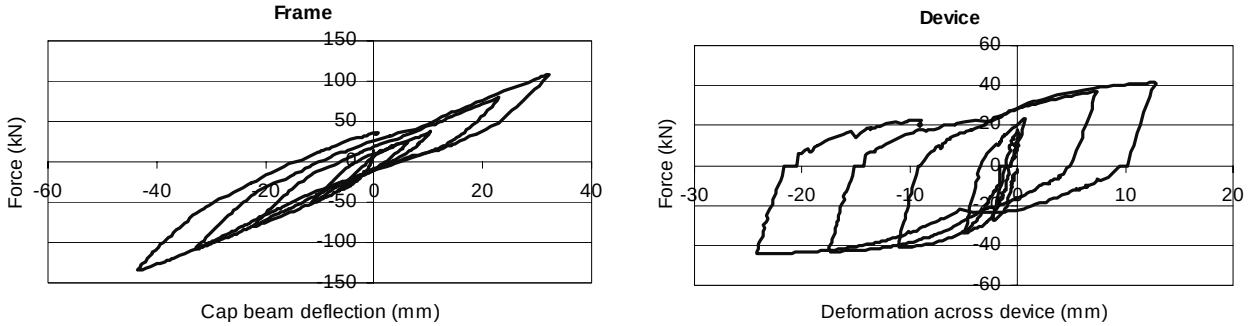

Figure 4.14. Cyclic test – 1.5 mm single plate

2 mm single plate (Test 19). Buckling became evident early in the 20 mm cycle, but the device went on to withstand a full cycle at ±40 mm. The device hysteresis loop shows a noticeable pinching at a small negative displacement, thought to be related to the transition from a buckle in one direction to the other.

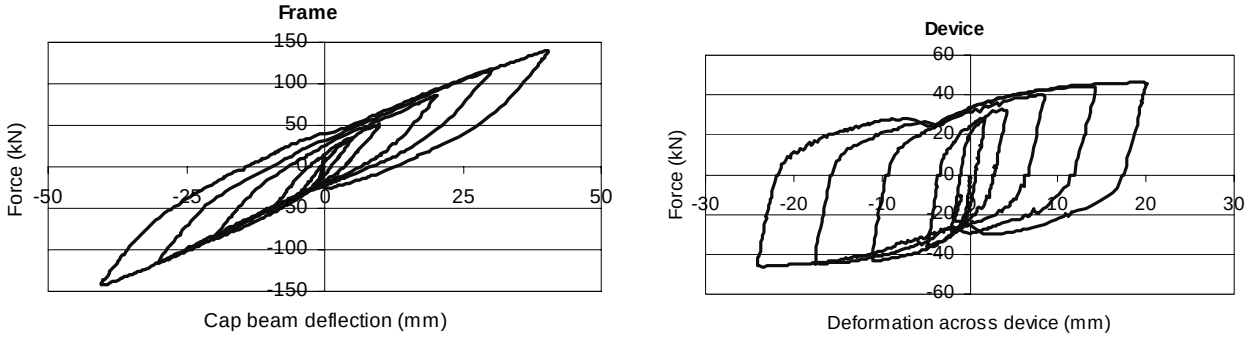

Figure 4.15. Cyclic test – 2 mm single plate

2 x 1 mm plates (Test 7). Buckling was visible from the 10 mm cycle onwards (significantly earlier than the single 2 mm plate), and the test was continued up to ±30 mm. Nevertheless, the device hysteresis loop is broadly similar to the single 2 mm plate case (compare Figures 4.15 and 4.16). Figure 4.17 shows the device at two different deformation amplitudes.

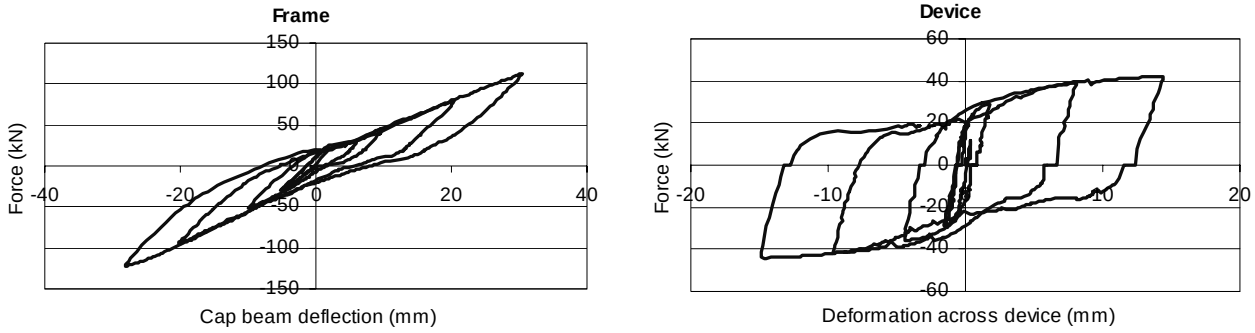

Figure 4.16. Cyclic test – 2 x 1 mm plates

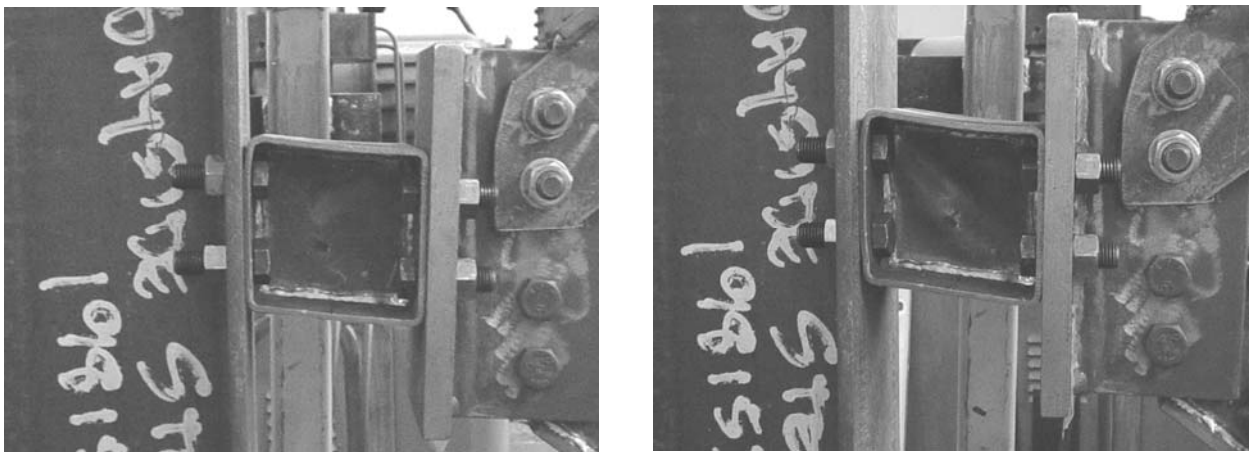

Figure 4.17. 2 x 1 mm plate device at upwards cap beam displacements of 20 mm (left) and 30 mm (right)

3 mm single plate (Test 22). A very shallow buckle developed on the second half of the ±40 mm cycle, but otherwise the device performed very well, exhibiting large, open hysteresis loops. The device response is again highly unsymmetrical, confirming that the asymmetry is not related to device buckling.

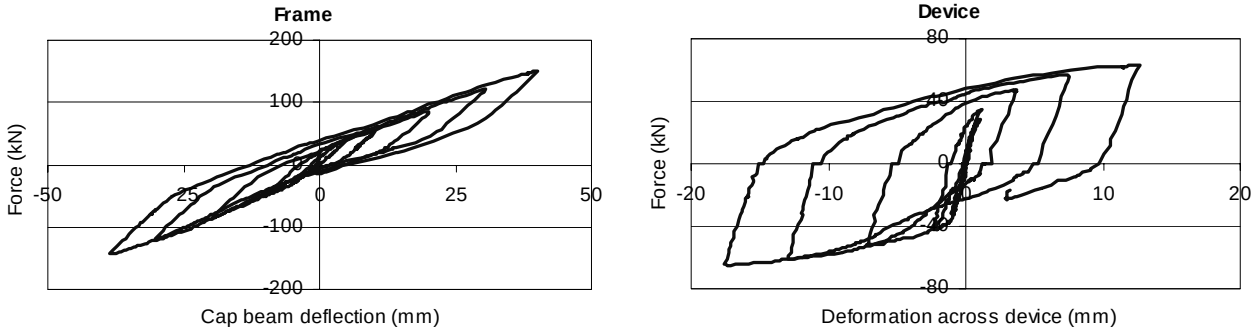

Figure 4.18. Cyclic test – 3 mm single plate

2 x 1.5 mm plates (Test 8). Buckling was visible from early in the 30 mm cycle onwards (significantly earlier than the single 3 mm plate), and the test was continued up to the first half of the 40 mm cycle. Peak loads and deformations were similar to those of the single 3 mm plate, but the hysteresis loops are rather narrower, implying less energy dissipation.

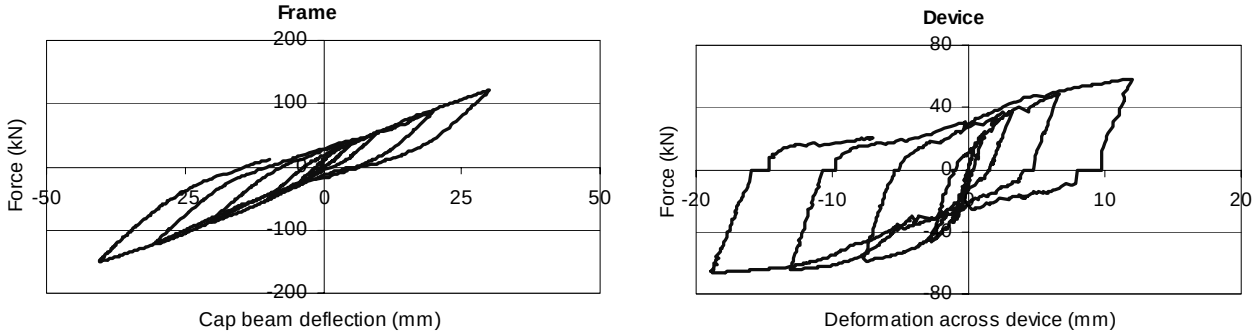

Figure 4.19. Cyclic test – 2 x 1.5 mm plates

4 mm single plate (Test 24). The test proceeded up to the first half of the 40 mm cycle, with no buckling evident at any stage. The device response was again highly unsymmetrical. This was the last test performed and there was some evidence that parts of the frame were deteriorating after being subjected to a large number of high-load cycles.

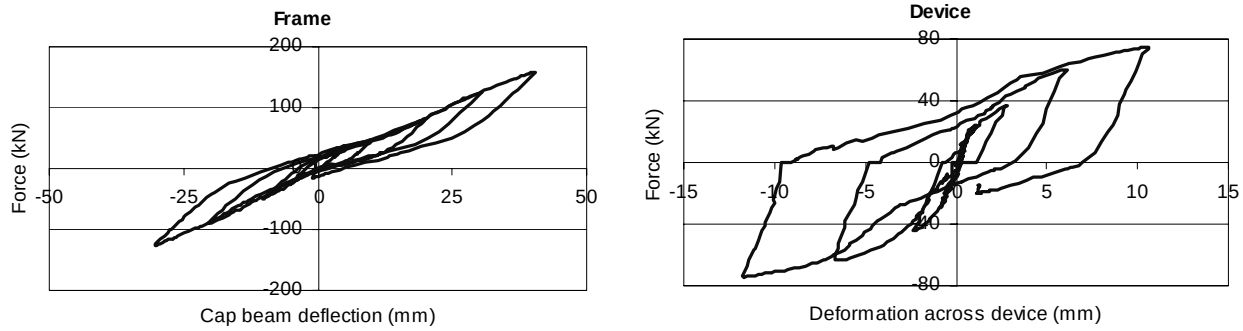

Figure 4.20. Cyclic test – 4 mm single plate

2 x 2 mm plates (Test 6). Buckling was visible from late in the 20 mm cycle onwards (compared with no buckling for the single 4 mm plate), and the test was continued up to the first half of the 40 mm cycle. Peak loads and deformations were similar to those of the single 4 mm plate.

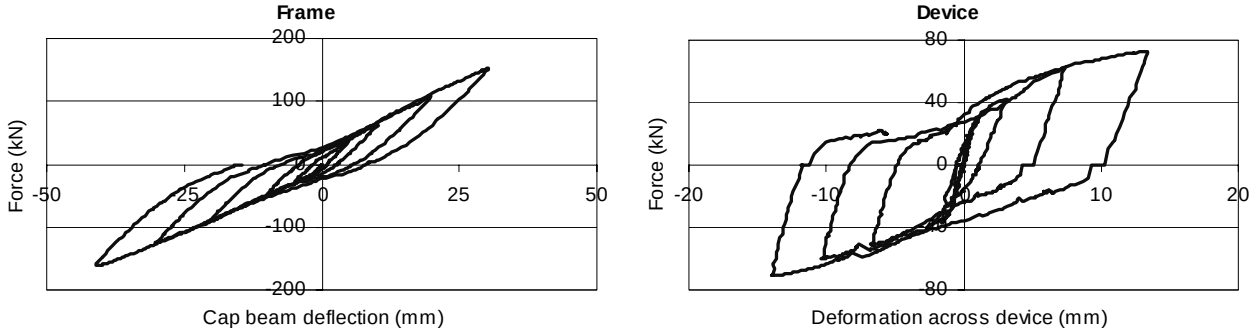

Figure 4.21. Cyclic test – 2 x 2 mm plates

4.1.4. Repeated cyclic tests

In these tests three reverse cycles were imposed at each displacement amplitude, from the 10 mm cycle onwards. The overall frame hysteresis plots showed very little deterioration between cycles and so added little to the single-cycle plots already presented. Therefore only the device hysteresis plots are presented here. The key indicates the cap beam displacement amplitude for each cycle.

1 mm single plate (Test 16). Some buckling occurred during the 5 mm cycles, and grew as the imposed displacements increased. Figure 4.22 shows the buckling state at three instants during the ±20 mm cycles. With the cap beam displaced 20 mm upwards a very severe top-left-to-bottom-right diagonal buckle is visible. Because the plate has been greatly stretched, the reverse buckle has formed by the time the device returns to its centre position. This buckle then amplifies as the device distorts the other way. The device failed by tearing along the welds at the top right and bottom left of the diaphragm while unloading at the end of the first ±30 mm cycle. The hysteresis loops in Figure 4.23 show very limited degradation between cycles, and large zero-load plateaus when unloading from the negative displacement cycles, thought to be due to flattening/reversal of buckles.

Figure 4.22. 1 mm single plate device during 20 mm cycles – from left to right:
end of upward stroke; device brought back to zero deformation; end of downward stroke

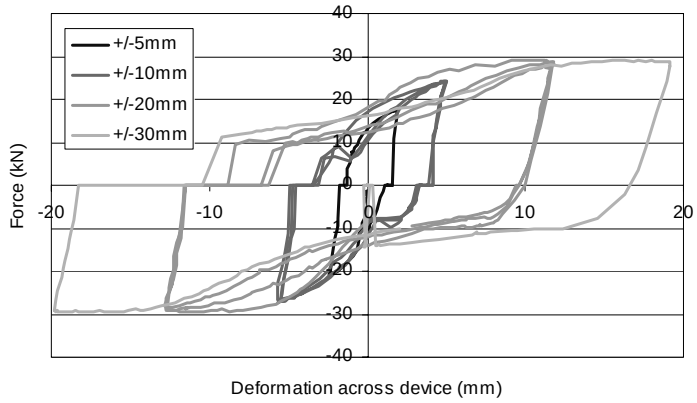

Figure 4.23. Device hysteresis in repeated cyclic test – 1 mm single plate

1.5 mm single plate (Test 15). Buckling was first noticed at an amplitude of 13 mm during the first 20 mm cycle. The device subsequently failed by tearing along a diagonal buckle line during the second 30 mm cycle. This test suffered a lot of bolt slip, resulting in rather noisy data.

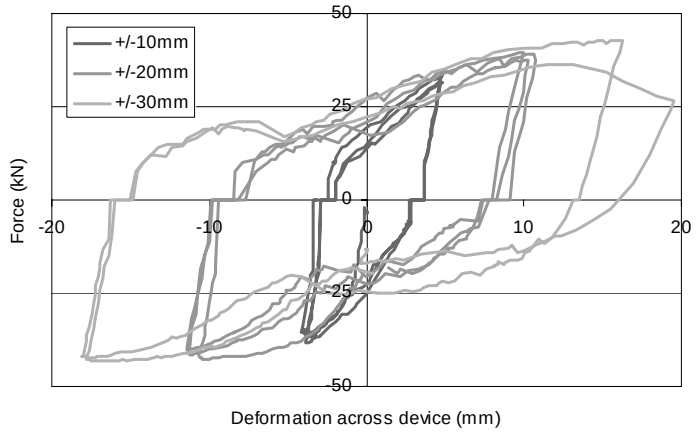

Figure 4.24. Device hysteresis in repeated cyclic test – 1.5 mm single plate

2 mm single plate (Test 20). Buckling was first noticed near the maximum of the first 20 mm cycle. No failure occurred. For most of the test a good degree of consistency was achieved between repeated cycles at a given amplitude.

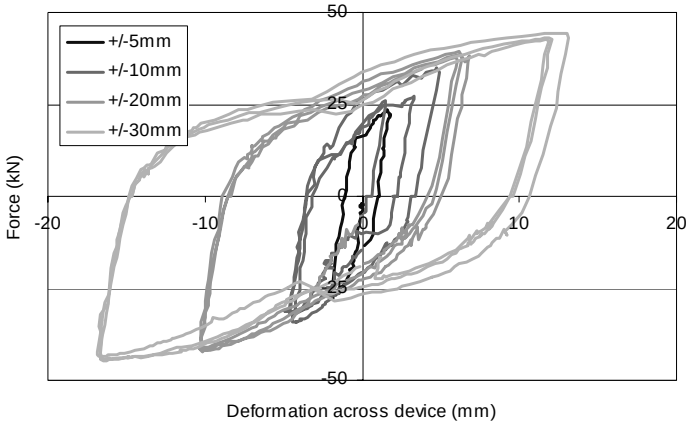

Figure 4.25. Device hysteresis in repeated cyclic test – 2 mm single plate

3 mm single plate (Test 23). The deformations imposed on the device were highly unsymmetrical over each cycle, but reasonably repeatable between cycles. Some deterioration occurred between cycles at a given amplitude. No buckling or failure occurred at cap beam displacements of up to 30 mm.

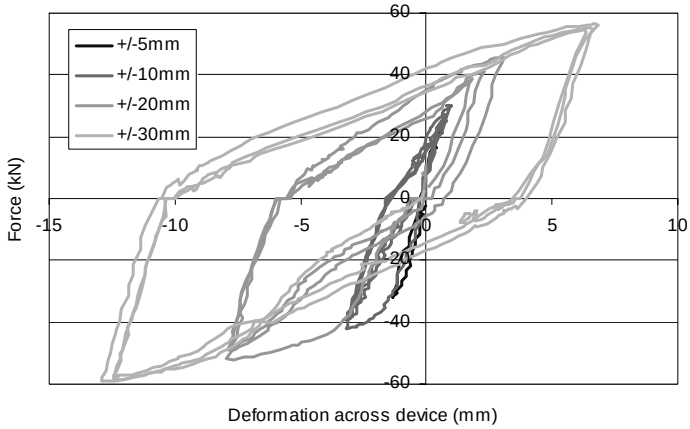

Figure 4.26. Device hysteresis in repeated cyclic test – 3 mm single plate

2 x 2 mm plates (Test 14). Buckled at around 25 mm displacement during first 30 mm cycle. Test suffered from quite large amounts of bolt slip. Test was aborted early in first 40 mm cycle as actuator load capacity was reached.

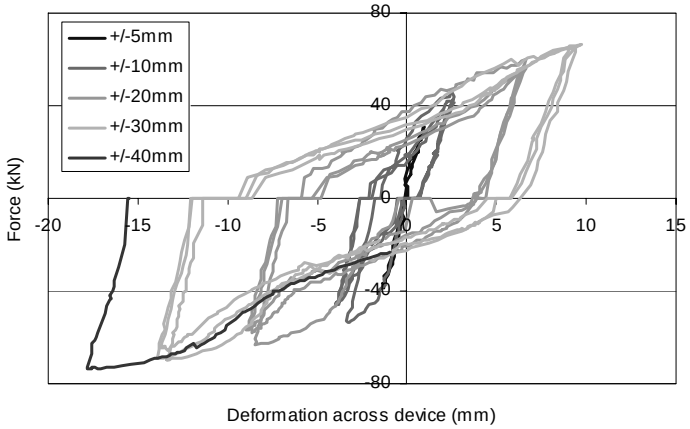

Figure 4.27. Device hysteresis in repeated cyclic test – 2 x 2 mm plates

4.2. Analysis of Monotonic Test Results

The monotonic test performance was broadly as expected, with both yield load and buckling load increasing with plate thickness. However, there were some differences between observed yield loads and those predicted by assuming simple shear yielding of the diaphragm plate. Table 4.1 shows experimentally deduced yield loads for the devices (deduced by fitting a best-fit bilinear curve to the date) and theoretical values.

Table 4.1. Experimental and theoretical yield loads for monotonic tests

Diaphragm thickness (mm)	Yield load (kN)	
	Experiment	Theory
1	18.5	10
1.5	28	24.9
2	28	26
2 × 1	32	19
3	32	42.8
2 × 1.5	41.5	49.8
4	43	60
2 × 2	40	52

Clearly the theory underestimates the yield load for the thinner plates, but overestimates it for the thicker ones. A possible explanation for the case of the thinner plates is that they are significantly strengthened by the confinement provided by the short length of box section, an effect ignored in the simple theoretical calculation. The reason for the overestimate in the case of the thicker plates is less clear, but this result possibly implies that the stress state in the plates is more complex than pure shear.

Another interesting point of comparison is the relative performances of single and double plate devices having the same effective thickness. Figure 4.28 shows comparisons up to the point of maximum load for effective thicknesses of 2, 3 and 4 mm. Clearly the differences in performance between equivalent devices are not great in a monotonic test, in spite of the fact that buckling was general observed at significantly lower deformations for single plate than for double plate devices.

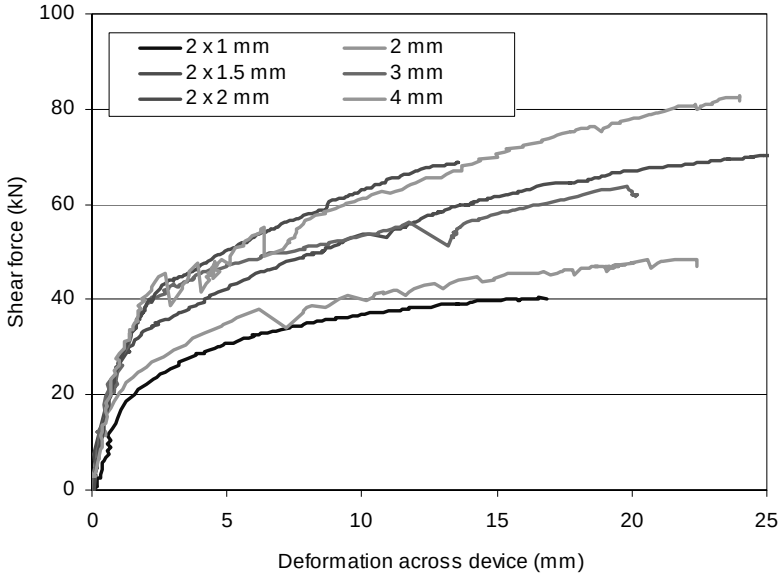

Figure 4.28. Comparisons of force-deformation characteristics of single and double plate devices

4.3. Cyclic Test Performance

The devices generally performed well in cyclic tests involving only a single cycle at each amplitude. Despite relatively early and repeated buckling of the thinner diaphragms, all devices remained stable up to frame displacement amplitudes of at least 30 mm, with no fracture or failure occurring in any case. In general, single-plate devices seem to have suffered less buckling and given slightly larger, more stable hysteresis loops than the equivalent double-plate devices, though the differences are not great.

To give some further insight into the relative performances of the devices and their influence on the frame behaviour, some further post-processing has been undertaken. First, the monotonic results were used to estimate yield forces and deformations, both for the frame as a whole, and for the force and deformation in the device itself. It should be noted that the yield deformations are quite difficult to estimate to a high degree of accuracy and, with the exception of the very thinnest device, did not show much variation between devices – the figures used are therefore approximate averages over a number of different devices. Using these results together with peak forces and deformations measured in the cyclic tests, it is then possible to estimate the load increase beyond yield and the ductility achieved. In each case, figures have been computed both for the frame as a whole and for the device in isolation. The results are shown in Table 4.2. Note that the maximum values achieved here are not ultimate values since no device actually failed – they are simply the maximum values reached before the decision was taken to stop the test.

Table 4.2. Force ratios and ductilities in simple cyclic tests

Plate Th. (mm)	F_y (kN)		u_y (mm)		F_{max} (kN)		u_{max} (mm)		F_{max}/F_y		μ	
	Fr.	Dev.	Fr.	Dev.	Fr.	Dev.	Fr.	Dev.	Fr.	Dev.	Fr.	Dev.
1	26	18.5	3.5	1.2	103.9	26.9	30.1	19.7	4.0	1.5	8.6	16.4
1.5	45	28	5.0	1.2	134.7	44.4	43.5	24.2	3.0	1.6	8.7	20.2
2	36	28	5.0	1.2	142.9	46.2	40.5	24.1	4.0	1.7	8.1	20.1
2×1	59	32	5.0	1.2	121.8	44.1	30.4	14.9	2.1	1.4	6.1	12.4
3	41	32	5.0	1.2	151.5	64.9	40.2	17.6	3.7	2.0	8.0	14.7
2×1.5	61	41.5	5.0	1.2	149.7	66.1	40.4	18.9	2.5	1.6	8.1	15.8
4	54	43	5.0	1.2	158.8	74.9	40.3	11.8	2.9	1.7	8.1	9.8
2×2	71	40	5.0	1.2	168.0	72.8	40.9	14.0	2.4	1.8	8.2	11.7

Firstly, it can be seen the devices strain harden significantly and so carry substantial additional load after first yield – up to double the yield load in one case. Any analysis that treats the device as elastic-perfectly plastic is likely to underestimate the loads on the structure by a large amount. Of course, with the main frame elements remaining elastic, the overall frame carries significantly more load after yield of the device – up to four times the load at the onset of yielding.

Turning to the ductilities, it can be seen that the thinner diaphragms sustain ductilities of the order of 20, while for thicker ones the maximum ductility in these tests was 10-15. In all cases the overall ductility of the frame (i.e. the ratio of peak cap beam displacement to the value at first yield) was around 8. Note that these figures are approximate, because of the difficulty in accurately estimating the yield deformations, as discussed above.

Another way of normalising the device deformations would be to calculate a shear strain. Since the plate dimension is 100 mm, the calculation is very simple – the plate deformation in mm is equal to the shear strain in %. So the diaphragms in these tests withstood maximum shear strains in the range 11.8 to 24.2% without fracturing.

4.4. Device Deformation and Hysteretic Energy Absorption

Since the key objective of a dissipative device is to absorb seismic energy, the measured energy dissipation is a key test parameter. This is quite easily calculated as the area within the hysteresis loops. The energy absorbed depends on both the size of the diaphragm and the amount of plastic deformation it sustains.

Figure 4.29 shows the diaphragm deformation as a function of its thickness for different cap beam displacement amplitudes. As would be expected, the thicker devices tend to undergo less deformation than the thinner ones for a given frame displacement. Figure 4.30 then shows the energy absorption plotted in the same way. This appears to show that the 2 mm diaphragm offers the best energy absorption capacity – thinner diaphragms buckle too easily and simply do not have as much material to deform, thicker ones are more resistant to yielding and so undergo less plastic deformation.

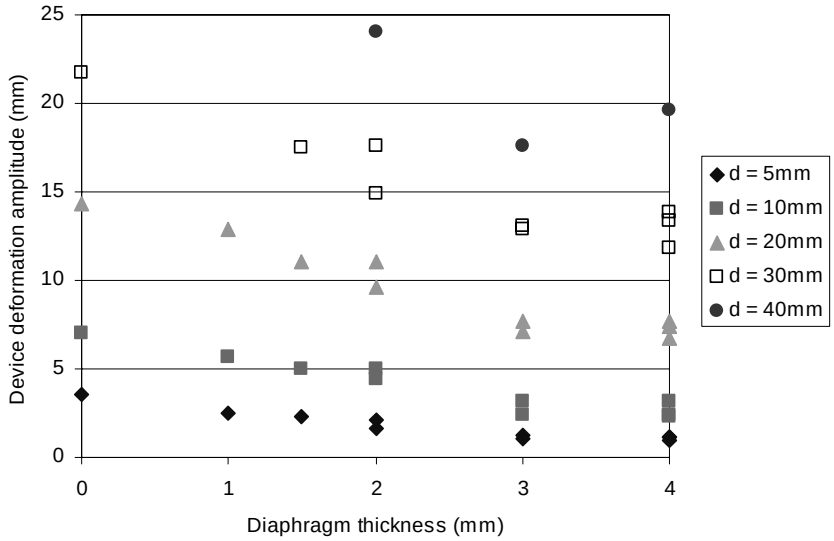

Figure 4.29. Device deformations at different cap beam displacement amplitudes

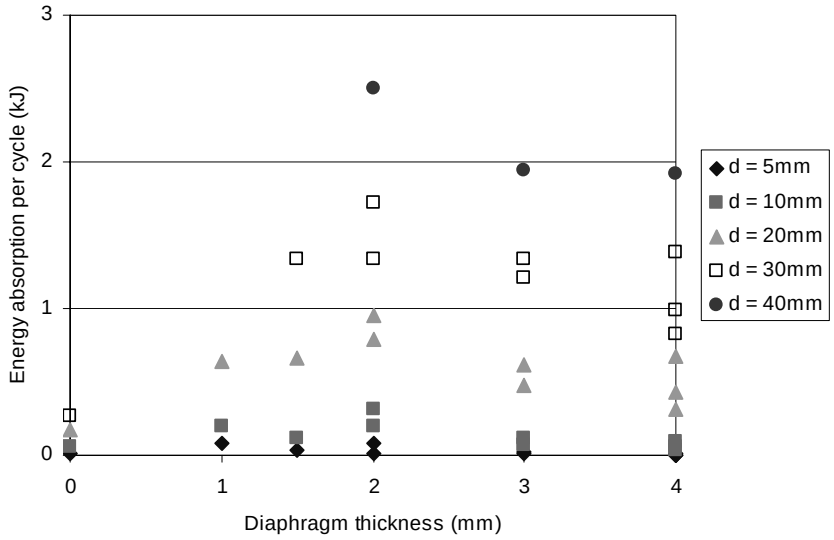

Figure 4.30. Energy absorption at different cap beam displacement amplitudes

An alternative presentation of the same data is shown in Figures 4.31 and 4.32, in which the energy absorption is plotted as a function of cap beam displacement and device deformation respectively. Figure 4.32 shows that, for a given device deformation, the thicker plates generally dissipate more energy. However, since thicker plates undergo less deformation for a given cap beam displacement, they may not be optimal. Figure 4.31 again suggests that the 2 mm diaphragms give the best energy dissipation for this frame, with the 3 mm diaphragms not far behind.

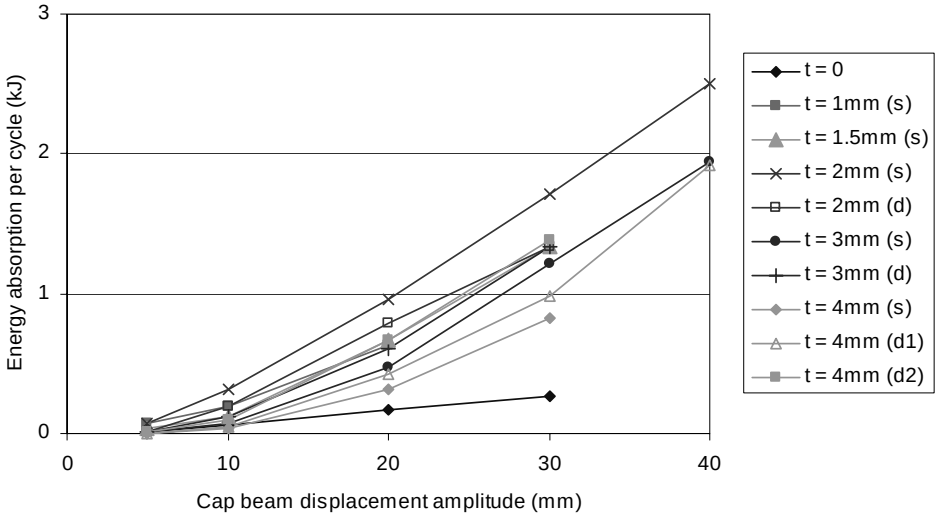

Figure 4.31. Energy absorption as a function of cap beam displacement amplitude (t = total plate thickness, s = single plate, d = double plate)

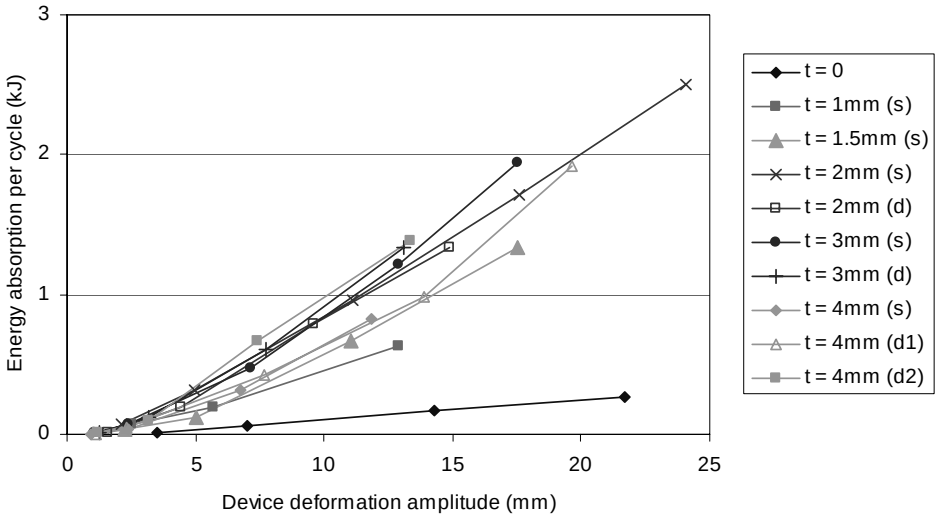

Figure 4.32. Energy absorption as a function of device deformation amplitude (t = total plate thickness, s = single plate, d = double plate)

The magnitude of the energy absorption is also worthy of comment. For the devices tested (100 mm square and up to 4 mm thick) the energy absorbed is of the order of 1-2 kJ per large-amplitude cycle. It is reasonable to assume that this figure would scale roughly proportionally for larger devices. To put this figure in perspective, a 100 tonne mass moving sinusoidally at 1 Hz with displacement amplitude 30 mm has a peak kinetic energy of 1.8 kJ. Clearly the devices possess sufficient energy dissipation capacity to make a significant impact on the performance of a building.

4.5. Comparison of Single-Cycle and Multi-Cycle Tests

In general, the device performance with three cycles at each amplitude was very similar to that with a single cycle at each amplitude – compare Figures 4.13 and 4.23, 4.14 and 4.24, 4.15 and 4.25, 4.18 and 4.26, 4.21 and 4.27. The devices mostly show very stable hysteresis loops, with only a small reduction in load between cycles at a given amplitude.

The important exceptions are the two thinnest plates tested. Both the 1 mm and the 1.5 mm diaphragms fractured during cycling at ±30 mm, presumably due to low cycle fatigue at the large plastic strains experienced. These are therefore clearly unsuitable. The 2 mm diaphragm did not fracture but did undergo large-scale plastic buckling, which gives rise to the risk of failure. The 3 mm diaphragm, however, showed no ill effects even under the most severe test regime. Since its energy absorption performance is close to that of the 2 mm device, the 3 mm device is considered to offer the best combination of energy dissipation and device stability. This represents a ratio of plate thickness to breadth of 0.03, a figure which may be transferable to other devices.

4.6. Comments on Performance of Tests and Possible Improvements

The tests were easy to perform. The bolted connections to the device suffered some slip but this did not appear to have a dramatic effect on the overall hysteresis response. The connections survived the test well and the devices were easy to remove and replace between tests, which is important for their practical use. However, there were some minor problems which could be reduced by a modest re-design of the rig before conducting further tests.

First, there was a noticeable asymmetry in many of the cyclic test results. The reasons for this have not been fully established, but are thought to be mainly due to the frame support conditions. In future it would be better if the rig could be rotated through 90° and mounted on a rigid base, with the actuator horizontal. The provision of proper, machined pin supports would also reduce the non-linearity.

In some tests, quite a large amount of longitudinal slip occurred at the brace connections near the device, and the bolt-holes in the brace connection plates became elongated in later tests. Some bolt slip is desirable to enable the connection to rotate and so not transfer moments into the braces. However, thicker connection plates and two lines of bolts would help to prevent the excessive slip that was observed in some tests. No slip is desirable in the connection of the device itself – it might therefore be advisable to use friction grip bolts for this connection.

Load in these tests was provided by a simple manually controlled actuator, which meant that the applied load/displacement and loading rate could not be controlled exactly. Although reasonably accurate control was achieved, the tests could be improved and automated if a servo-controlled actuator could be use, with electronic control based on either load or displacement.

The tests performed here represent a start to a fuller investigation of these devices. Only a single overall device size (100 mm square) has been studied, together with a variety of diaphragm thicknesses. To investigate the size dependency, at least two further device sizes should be studied.

Lastly, the device performance has not proved completely predictable and greater insight could be achieved through detailed, non-linear finite element modelling of a device under both monotonic and cyclic loads.

5. CONCLUSIONS

1. A quite extensive series of tests on 100 mm square dissipative devices has been successfully performed. The simple setup proved reasonably robust and repeatable, though some improvements have been suggested in section 4.6.

2. The devices were easy and cheap to manufacture, fit, remove and replace. They therefore have the potential to offer practical, low-cost protection to buildings.

3. All the devices tested yielded at quite low deformations and sustained very large ductilities (greater than 10) without failure. This suggests that they would begin to dissipate energy early in an earthquake, and would continue to do so as the earthquake motion increased.

4. The load carried by the device continued to increase after yield, with a ratio of maximum force carried to yield force of around 1.7 in most tests.

5. While a device with a 2 mm diaphragm appeared to offer the maximum energy dissipation capacity, thinner devices are prone to buckling and to fracture under repeated, large-amplitude cycling. A thickness of 3 mm (i.e. thickness to breadth ratio of 0.03) is recommended as offering the best combination of dissipative capacity and robustness.

6. A 3 mm device dissipated approximately 1.3 kJ of energy when the frame in which it was fitted underwent a single displacement cycle of amplitude 30 mm.

REFERENCES

[1] AS 4100 – 1990. *Steel structures*. Australian Standards Association, Homebush NSW, Australia.
[2] Blackeborough, A., Williams, M.S., Darby, A.P. and Williams, D.M., "The development of real-time substructure testing", Philosophical Transactions of the Royal Society of London, Series A, 2001, 359(1786), 1869-92.
[3] OneSteel, Structural steel products tables, 2003. www.onesteel.com
[4] Zieman, R.D. and McGuire, W., "Mastan 2 Version 1.0", Wiley, New York, 2000.